Instantaneous interactions between brain sites can distinguish movement from rest but are relatively poor at resolving different movement types

Kai J. Miller-*IEEE Member*, Jeffrey G. Ojemann, and Jaimie M. Henderson

Abstract— **Classification of finger movements from brain signals is an important problem in emerging neural prosthetics research. Current techniques have focused primarily on aggregating data from different brain sites independently, without regard to the interaction between different brain sites. We performed a very simple experiment classifying finger movements during electrocorticographic recording from motor cortex. Unlike previous experiments of this type, we examined whether the most-simple type of instantaneous interactions between brain regions could improve classification. We focused on two simple, but salient markers: phase coherence of the 12-20 Hz beta range, and simple correlation in broadband spectral change. We compared behavioral classification using these interactions with simple amplitude changes in beta and broadband magnitude. We found that inter-electrode phase coherence and cross-correlation, were relatively poor at distinguishing between finger movements, and only mediocre at identifying null/rest periods.**

I. Introduction

Human motor behaviors such as reaching, grasping and speaking, are executed and controlled by the sensorimotor regions of the cerebral cortex, which are located immediately anterior and posterior of the central sulcus. This peri-central system is known to manifest a 12-20 Hz electrical oscillation known as the beta rhythm. The cortical surface beta rhythm has long been known to have an inverse relation to sensory processing and motor production. The peri-central beta rhythm is decreased during movement initiation and production (illustrated in figure 1), and during motor imagery [1-3].

Because rhythmic (band-limited) and non-rhythmic (broadband) components of the power spectrum have distinct frequency profiles and exhibit distinct task-related changes, they can be decoupled from one another [4]. While previous studies have focused on the classifiability of rhythmic and broadband amplitude changes [5], there is increasing attention to the interactions between brain regions during motor movements and brain computer interfacing [6]. We examined whether the most-simple type of instantaneous interactions between brain regions could be used for classification. We focused on two simple, but salient markers: phase coherence of the 12-20 Hz beta range, and simple correlation in broadband spectral change.

Research supported by the generous contribution of NASA GSRP (KJM); NSF 0930908 (JGO); and NIH R01-NS065186 (KJM, JGO).

Kai J Miller and Jaimie Henderson, Department of Neurological Surgery, Stanford University, 300 Pasteur Lane, Stanford, CA, 94305 USA (650-723-4000, kai.miller@stanford.edu).

Jeffrey G. Ojemann, Department of Neurosurgery, University of Washington, 1959 NE Pacific, Seattle, WA 98195

II. Experimental Methods

A. Human subjects:

Seven patients participated in the study, and all were patients at Harborview Hospital in Seattle, WA, USA. Each had sub-dural platinum electrocorticographic (ECoG) grids placed for extended clinical monitoring and localization of seizure foci, in the course of the treatment for medically-refractory epilepsy. All patients participated in a purely voluntary manner, after providing informed written consent, under protocols approved by the Institutional Review Board of the University of Washington. Finger position was recorded using a sensor dataglove. ECoG signals were acquired from the experimental amplifiers using the general-purpose BCI2000 software [7], which was also used for stimulus presentation. Electrode localization and mapping was performed using [8]. Data are from prior study [4, 9].

B. Task

Subjects were cued with a word displayed on a bedside monitor indicating which finger to move during 2-second movement trials, with interleaving rest periods, while wearing a dataglove. The subject performed self-paced movements in response to each of these cues, and they typically moved each finger ~2-5 times during each trial (~0.4-1.0s per movement), although some varied. For blocks of behavior, the subjects were able to move the appropriate finger during the cue, but usually exceeded the cue time, moving into the following rest period. Therefore, there were typically ~30 rest epochs that met our inclusion criteria of 1.5s in length that could be used for analysis, so the number of finger movement blocks of any given type and the number of rest blocks was approximately the same.

III. Signal Processing

To reduce common artifact, the raw potential was common-average re-referenced, after electrodes with significant artifact or epileptiform activity had been rejected.

A. Isolating the timecourse of the beta rhythm:

A complex signal to reflect the timecourse of a functionally-relevant frequency-range band was constructed as follows: The signal $V(t)$ was band-passed using a 3rd order Butterworth filter for a specific range, to obtain the "band-limited" potential, $V(F,t)$, where F denotes the frequency range (e.g. for "beta", $F \rightarrow$ [12-20Hz], etc.). A complex, analytic, signal, $\tilde{V}(F,t) = V(F,t) + iV^{IM}(F,t)$, was constructed using the Hilbert transform, also dentoed

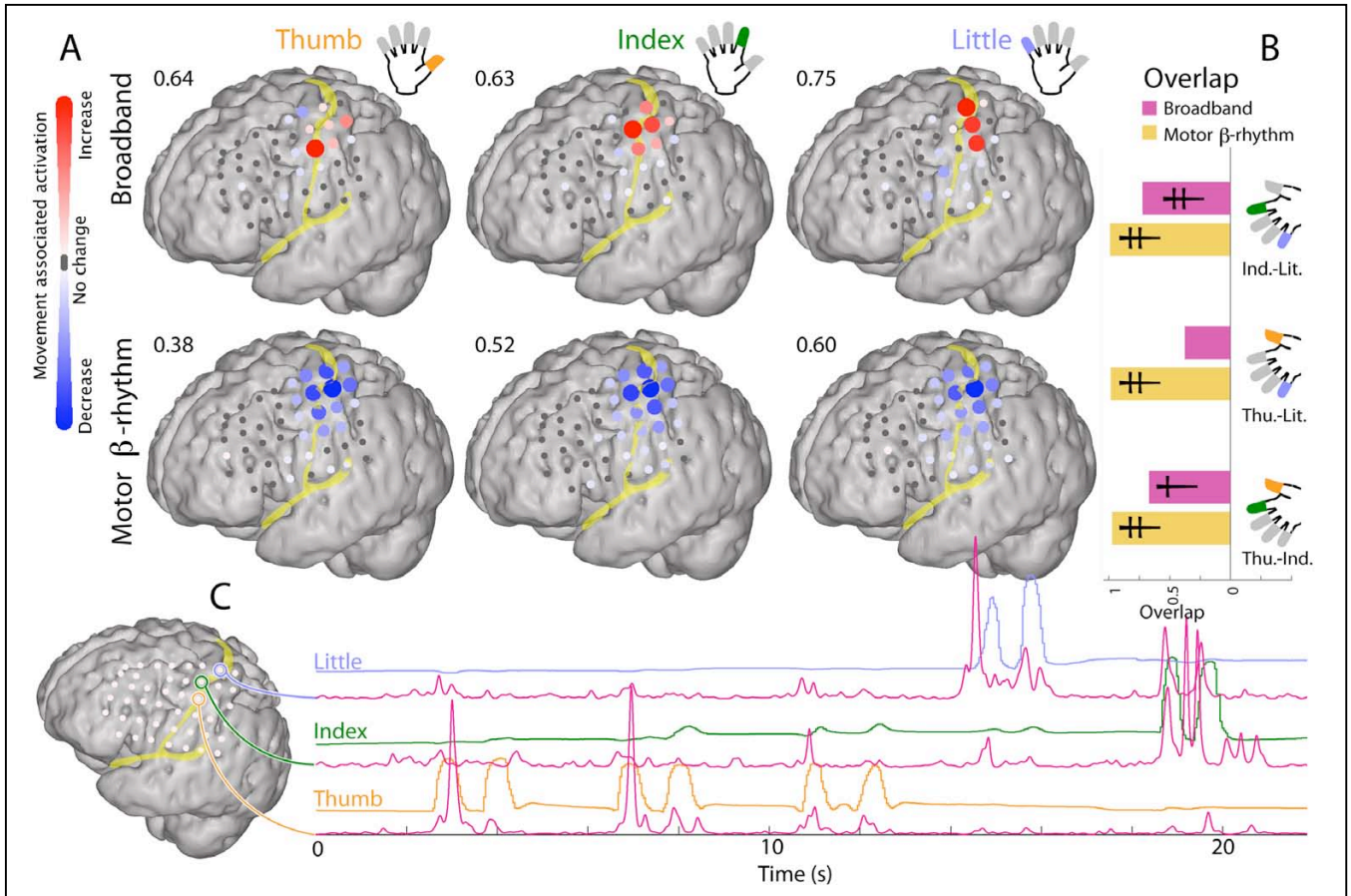

Figure 1: ECoG broadband power resolves somatotopic representation of fingers (Subject 1). (A) Changes in broadband and 12-20Hz beta power at different cortical sites for movement of thumb, index, and little finger. Colors denote a signed r^2 measurement of increases and decreases in power with movement relative to rest (individually scaled with maximum to upper left of each plot). Electrode arrays were spaced at 1cm (standard clinical arrays). **(B)** Quantification of spatial overlap between changes associated with finger-movements. (1 is maximum possible overlap and 0 is no overlap; negative overlaps occur when increases overlap with decrease). Resampling significance (by randomly shuffling electrode labels), single cross denotes $p<0.01$, double denotes $p<0.001$, that the overlap happened by chance. **(C)** Traces of thumb (orange), index (green), and little finger (light blue) position, with corresponding timecourse of broadband spectral change (see methods) for 3 cortical sites.

$\tilde{V}(F,t) = r(F,t)e^{i\phi(F,t)}$. The "analytic amplitude" of the range F at time t is $r(F,t)$ and the "phase" is $\phi(F,t)$. The single trial average rhythm magnitude is the average of this analytic amplitude: $r(F,q) = \langle r(F,t) \rangle_{t \in q}$. Because only the $F \rightarrow$ [12-20Hz] beta range is used, F is dropped from further notation. Note that all filtering was done bi-directionally.

B. *Isolating the timecourse of broadband spectral shift:*

From each electrode, samples of power spectral density (PSD) were calculated from 1 second epochs centered at the peak displacement of each finger movement, or from random points during rest periods. Individual PSDs were normalized in two steps: each spectral sample was element-wise divided at each frequency by the average across the ensemble of all epochs, and then the log was taken. A matrix from the inner product of these PSDs was then diagonalized via a singular value decomposition, to identify motifs of movement-related change in the PSD. The eigenvectors (principal spectral components – "PSCs") from this decomposition reveal motifs in change in the PSD during cortical processing, and are ordered according to magnitude of the corresponding eigenvalue [4].

Continuous time-frequency approximations (dynamic spectra) were calculated using complex Morlet wavelets, which were then normalized by division of the mean power at each frequency and then taking the log. The timecourse of broadband spectral change was obtained by projecting the 1st PSC to this normalized dynamic spectrum (excepting 5Hz notches at 60Hz harmonics).

There is a power law in the cortical PSD of the form $P(f,t) = A(t) f^{-\chi}$, which is revealed by broadband fluctuations in the PSD across all frequencies (separate from the classic θ, α, and β rhythmic motifs) [4, 10]. This broadband (which we denote $\chi(t)$, with trial average $\chi(q)$) approximates the timecourse of multiplicative scaling in the timecourse of the power-law coefficient, $A(t)$, and when simulated, may be directly correlated with multiplicative factor in the average neuronal population firing rate [10].

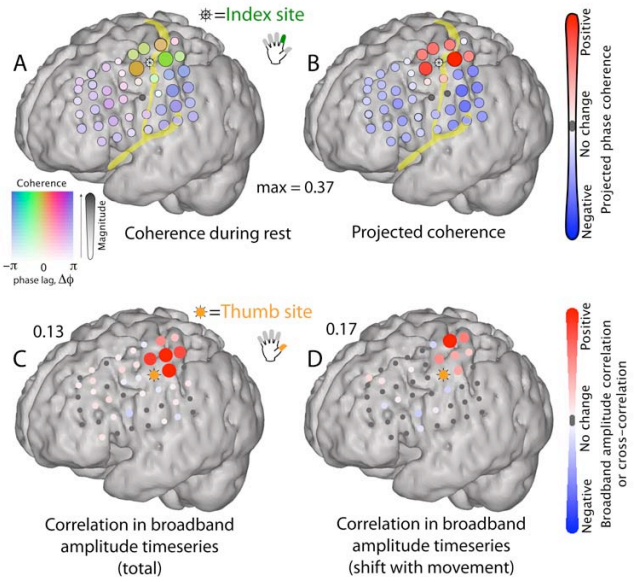

Figure 2: Illustration of pair-wise 12-20 Hz coherence, as well as pair-wise broadband timeseries correlation. (A) An index-finger specific site is identified by magnitude of broadband shift, and denoted with a "ship wheel" symbol. The pair-wise phase coherence between sites is calculated with the remainder of the array. The magnitude of the coherence is reflected in the strength of the color and the electrode diameter, whereas the relative phase-lag of the phase coherence is denoted by the color. **(B)** The coherence from each electrode site is projected onto the phase angle of maximum coherence. These projected values from each trial are used as features for the classifier. **(C)** Correlation between the thumb-selective site and the remainder of the array. Maximum 0.13. **(D)** Cross-correlation (r^2) between trials of inter-electrode broadband correlation (Max 0.17).

C. *Trial-by-trial phase coherence of rhythms*

The pair-wise phase coherence relative to a reference site was examined. For the complex rhythm $\tilde{V}_a(t) = r_a(t)e^{i\phi_a(t)}$ (electrode a), the complex phase coherence [11] with other electrodes b, on trial q, is: $Q_{ab}(q) = \frac{1}{T}\sum_{t\in q} e^{i(\phi_a(t)-\phi_b(t))}$. The "seed" electrode ($a$) is one with the strongest index finger movement-associated broadband change. The complex portion was initially retained because, in the setting of a dominant, distributed, rhythm, the choice of common average reference introduces phase coherence with regions where the rhythm is otherwise absent. However, introduced coherence will be approximately π radians out of phase with the dominant rhythm. In order to obtain reliable statistical measure of coherence, each single-trial coherence was projected onto the average phase coherence angle for that movement type or rest, in that channel.

D. *Trial-by-trial broadband timecourse correlation*

The pair-wise correlation in broadband timecourse, $\Upsilon_{ab}(q)$, between several seed sites a and each other site b was similarly calculated for each movement or rest epoch. It was obtained as the simple correlation of $\chi_a(t)$ and $\chi_b(t)$ over the interval $t \in q$. Υ_{aa} excluded.

IV. Classification

Feature spaces were generated using single trial beta rhythm amplitude - $r(q)$, broadband amplitude $\chi(q)$, beta phase coherences $Q_{ab}(q)$, and broadband timecourse correlations Υ_{aa}. For the sake of simplicity, Fisher linear discriminant analysis (LDA) was used for classification [12]. The datapoints were divided into thirds, and three-fold cross-validation was applied (training on 2/3 and testing on the other). All individual features were first tested in the training set – if they did not distinguish at least one finger movement type from rest with r^2>.1, they were excluded from the classification feature space. PCA was applied to the coherence and cross-correlation sets for dimensionality reduction, to ensure that the covariance matrix for LDA remained positive definite.

V. Results

A. *Beta and broadband amplitudes*

As seen in figure 1, ECoG broadband resolves somatotopic representation of fingers quite well, and captures the dynamics of individual finger movements with high temporal precision. The beta rhythm, however, is overlapping between all movement types [4, 9]. When blocks of movement were classified based upon these features, individual finger movements and rest could be distinguished from one another very accurately (figure 3).

B. *Beta coherence*

Beta rhythm coherence obeys sulcal boundaries and is relatively confined to the dorsal rolandic cortex (figure 2 and [9]). Figure 3 (row 2) shows that rest can usually be distinguished from movement in most cases, but different finger movements generally cannot be resolved.

C. *Broadband cross-correlation between electrodes*

Simple broadband cross-correlation between electrodes, as illustrated in figure 2, is more tightly constrained to rolandic cortex than coherence is. However, it does not separate movement from rest as well as beta coherence does.

D. *Broadband cross-correlation and beta coherence combined*

As seen in figure 3, the synthesis of the two inter-electrode features results in mildly improved classification of different figures for subjects 1-4, but this effect is quite subtle. While the null/rest state is often able to be distinguished from different finger movements, this is only a very small improvement beyond using coherence alone.

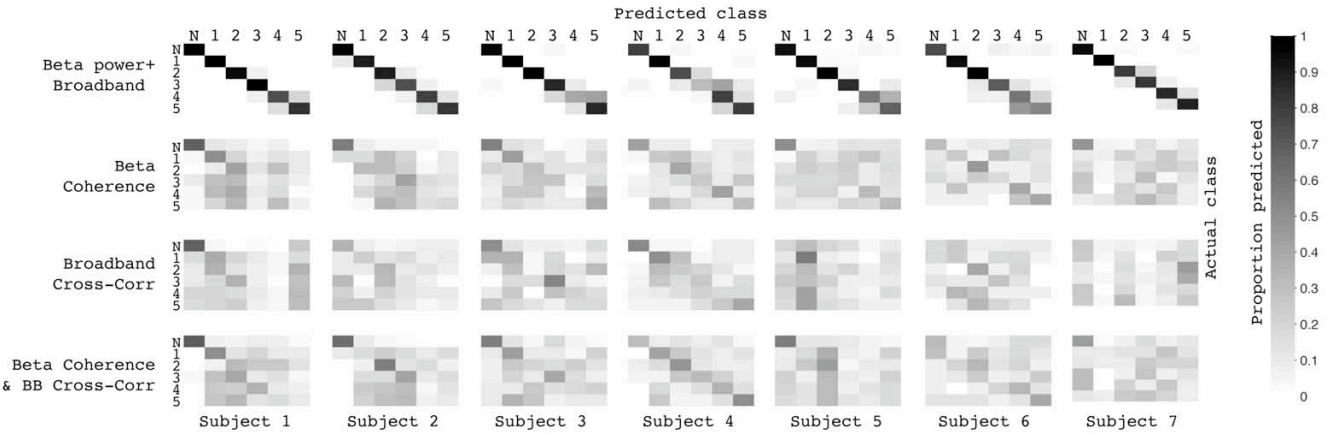

Figure 3: Predicted class vs actual class for different feature subgroups. The predicted finger movement behavior is shown on the horizontal axis, compared with the actual class. N=null/rest, 1=thumb, 2=index, 3=middle, 4=ring, 5=little. For the top row, beta and broadband amplitudes are used. As demonstrated in earlier studies, these can be predicted with very high accuracy. The second row shows classification when only beta coherence is used The third row shows classification result when only broadband amplitude cross-correlation is used. The fourth row shows classification when both beta coherence and broadband amplitude cross-correlation are used.

VI. Discussion

In this study two phenomena in the ECoG signal – broadband spectral change and the beta rhythm – were examined. As shown in previous studies, the magnitude of these phenomena can very robustly distinguish between different movement types and null/rest. However, the most commonly used metrics for characterizing the instantaneous interaction between electrodes, inter-electrode phase coherence and cross-correlation, were relatively poor at distinguishing between finger movements, and only mediocre at identifying null/rest periods. These findings may have been expected for a number of reasons.

The coherence effect would have been expected to be different for movement vs rest only, because beta rhythm power changes as well as beta rhythm resting coherence are both gyrally constrained, and strongly overlapping [9]. Although the coherence measure is independent of these power changes, the ability to quantify the phase of the rhythm is better at higher amplitudes, so the coherence measure may just be more reliable when the patient is resting. Because the beta rhythm has been shown to be a spatially coherent 'module' in motor cortex, that is diminished during movement, it may be that the module is less likely to be characterized while moving (rather than there being a difference in information transfer between regions).

Broadband shifts can then be understood as a change in the amplitude of a non-rhythmic, stochastic, process, which reflects the dendritic integration of asynchronous inputs – i.e. they are a reflection of mean firing rate. We might expect there to be very significant correlations in firing rate between brain regions during the planning and execution of movements, that are different for different types of movement. However, we did not see marked differences in this study. The most likely explanation for this is that the instantaneous cross-correlation was used, and information is not transferred instaneously. Rather, future studies should begin with delayed cross-correlation between regions to allow for the fact that information transfer takes time. Using a very simple classification approach, this work demonstrates that even the simplest characterization of instantaneous interactions between brain regions can be used for classification, but only weakly. It serves as a basic starting point for further work into inter-regional brain interactions and their role in brain-machine interfacing.

Acknowledgment

We appreciate the time and dedication of the patients and staff at Harborview Hospital in Seattle, WA, USA.

References

[1] Miller, K.J., et al., *Spectral changes in cortical surface potentials during motor movement.* J Neurosci, 2007. **27**(9): p. 2424-32.
[2] Miller, K.J., et al., *Cortical activity during motor execution, motor imagery, and imagery-based online feedback.* Proceedings of the National Academy of Sciences, 2010. **108**(9): p. 4430-4435.
[3] Hermes, D., et al., *Neurophysiologic correlates of fMRI in human motor cortex.* Hum Brain Mapp, 2012. **33**(7): p. 1689-99.
[4] Miller, K.J., et al., *Decoupling the Cortical Power Spectrum Reveals Real-Time Representation of Individual Finger Movements in Humans.* Journal of Neuroscience, 2009. **29**(10): p. 3132.
[5] Chestek, C.A., et al., *Hand posture classification using electrocorticography signals in the gamma band over human sensorimotor brain areas.* J Neural Eng, 2013. **10**(2): p. 026002.
[6] Wander, J.D., et al., *Distributed cortical adaptation during learning of a brain-computer interface task.* Proc Natl Acad Sci U S A, 2013. **110**(26)
[7] Schalk, G., et al., *BCI2000: a general-purpose brain-computer interface (BCI) system.* IEEE Trans Biomed Eng, 2004. **51**(6): p. 1034-43.
[8] Hermes, D., et al., *Automated electrocorticographic electrode localization on individually rendered brain surfaces.* Journal of neuroscience methods, 2010. **185**(2): p. 293-298.
[9] Miller, K.J., et al., *Human motor cortical activity is selectively phase-entrained on underlying rhythms.* PLoS Comput Biol, 2012. **8**(9):
[10] Miller, K.J., et al., *Power-law scaling in the brain surface electric potential.* PLoS computational biology, 2009. **5**(12): p. e1000609.
[11] Lachaux, J.P., et al., *Measuring phase synchrony in brain signals.* Human brain mapping, 1999. **8**(4): p. 194-208.
[12] Russel, S. and P. Norvig, *Artificial Intelligence: a modern approach*. 2003: Prentice Hall.